

EFFICIENCY IN ELECTRO-FENTON OXIDATION OF CTMP PULPING WASTEWATER

QIANG ZHAO, XUEMING ZHANG, DEZHI SUN, XIAOJUAN JIN and ZHAOHONG WANG

*College of Materials Science and Technology, Beijing Forestry University,
Beijing, 100083, P.R. China*

✉ *Corresponding author: Qiang Zhao, zhaoqiang@bjfu.edu.cn*

Received December 1, 2017

Wastewater originating from chemithermomechanical pulping (CTMP) contains various organic compounds and therefore it is difficult to treat. To increase the effect of oxidation, the electro-Fenton process was employed in this study. Fenton's reagent (H_2O_2 and Fe^{2+}) was produced by simultaneous reduction of O_2 and Fe^{3+} on a stainless cathode in an acidic medium. Electrochemistry combined with Fenton's reagent provides the hydroxyl radical, a powerful oxidant. The chemical oxygen demand (COD) removal efficiencies and the turbidity of electro-Fenton oxidation on preimpregnated wastewater of CTMP were investigated. The optimal electro-Fenton oxidation conditions were determined as follows: pH 4, applied voltage of 12 V, current of 0.2 A, electrode space of 2 cm and aeration gas flow of 16 L/h. The COD_{cr} removal rate could reach 40.1% and the turbidity removal rate achieved by the aforementioned electro-Fenton process was 49.9%. Fourier transform infrared spectroscopy showed that electro-Fenton oxidation induced higher degradation of preimpregnated wastewater of CTMP than Fenton oxidation alone.

Keywords: Fenton oxidation, electro-Fenton, CTMP, preimpregnation wastewater, FTIR

INTRODUCTION

A comparison of different sources of pulping fibers indicates that wood is the most abundant source of papermaking fiber. Wood compounds, including lignin, carbohydrates and extractives, are difficult to biodegrade and are washed away from the fibers during washing, dewatering and screening.¹ A large number of organic compounds have been identified in pulp mill effluents, some of which may be carcinogenic and mutagenic, such as dioxins, furans and polycyclic aromatic hydrocarbons. Pulp mill effluents also contain inorganic ions, organic polymers and biopolymers.² Color is largely caused by lignin and lignin derivatives, as well as by polymerized tannins, because of the presence of carbon-to-carbon biphenyl linkages.³⁻⁶

Electrochemical treatment of wastewater is considered one of the advanced oxidation processes and is a potentially powerful method of pollution control with high removal efficiencies.⁷ Electrochemical oxidation exhibits efficient and economical removal of dyes and highly efficient degradation of hard-to-treat pollutants.⁸ Thus, color reduction of about 100% can be achieved by electrolysis during only 6 min.⁹

Manisankar studied the decolorization of the dye effluent by electrochemical oxidation, using a lead dioxide-coated anode.¹⁰ Jethva found the electrochemical method to be effective in the removal of color and COD_{cr} reduction of azo dye effluents originating from two leading textile industries, using a flow reactor. Maximum color removal (95.2%) was achieved at a flow rate of 5 mL/min and current density of 29.9 mA/cm².¹¹

Focus has been recently directed towards electrochemical technology for its application in the wastewater treatment.^{12,13} The electro-Fenton technique has an advantage over the conventional Fenton process in process control and prevention of storage and transport of H_2O_2 . Moreover, the electro-Fenton method uses a clean energy source, preventing secondary pollutants.¹⁴ With this approach, highly reactive hydroxyl radicals are produced from electrochemically-assisted Fenton reaction between electro-generated ferrous iron and hydrogen peroxide.¹⁵ This combination of Fenton and electro-Fenton processes was proposed as an excellent choice for pulp and paper wastewater treatment.¹⁶⁻¹⁹

The present study mainly aimed to evaluate

the efficiency of the electro-Fenton treatment for the removal of organic compounds from preimpregnated CTMP wastewater, particularly those compounds that contribute to the COD, chroma and turbidity of wastewater.

EXPERIMENTAL

Chemicals

Sulfate, H₂O₂ (30%), FeSO₄·7H₂O (purity 99%), NaCl (purity 99%), ether and other chemicals of laboratory reagent grade were used without further purification. All the chemicals were purchased from Beijing Chemical Works and Beijing Yili Fine Chemicals Co., Inc. (China). All the solutions were prepared using high-purity deionized water.

Wastewater characterization

The wastewater sample was collected from the preimpregnation stage of CTMP pulping performed at a laboratory scale. The preimpregnation conditions were as follows: 4% NaOH, 4% Na₂SO₃, liquid ratio of 1:5, target temperature of 130 °C and holding time of 20 min. The wastewater samples were characterized as follows: pH 10.3, COD_{cr} of 21556.3 mg·L⁻¹, chroma of 62500 times and turbidity of 1680 NTU.

Wastewater analysis

Chemical oxygen demand (COD) analyses were conducted using a HATO @CTL-12 COD tester. Oxidation of CTMP preimpregnation wastewater was conducted using potassium dichromate in a concentrated acidic medium with silver sulfate as catalyst and mercury sulfate.

The chroma of the wastewater was tested by multiple dilution in accordance with the GB11903-89 standard. The turbidity of wastewater was evaluated using a high-turbidity tester (WZS-185).

GC/MS analysis

GC/MS analysis was conducted under the following conditions: chromatographic column – HP5MS quartz capillary column, column length – 30 m, inner diameter of the column – 0.25 mm, film thickness – 0.25 μm. Chromatographic separation was conducted under the following conditions: column temperature – 50 °C (retention time – 5 min) → 8 °C·min⁻¹ → 280 °C (retention time – 10 min), injection port temperature – 250-300 °C, vaporization temperature – 280 °C, carrier gas (flow) – He (1.0 mL·min⁻¹), split ratio – 50:1, injection volume – 1 μL.

Mass spectrometry and detection were performed under the following conditions: electron ionization source of 70 eV, source temperature of 230 °C, scanning range of 35-500 atomic mass units, scanning time of 1 s·scan⁻¹.

FTIR-ATR

Fourier transform infrared spectroscopy (FTIR)

was conducted using a Tensor 27 FTIR spectrometer. Infrared absorption spectra were recorded in the 4000-400 cm⁻¹ region.

Experimental methods

The apparatus, including an adjustable DC Power Supply (JS-5A), was used and operated in a plastic cube cell of 100 mL useful volume. Different electrode materials, such as stainless, iridium–ruthenium alloy and titanium mesh cathode, with a rectangular shape (6 cm × 5 cm × 1.5 cm), were used as cathodes, whereas a commercial stainless electrode was used as an anode. The COD_{cr}, chroma and turbidity of wastewater were tested after it was allowed to stand for 30 min.

All the reagents, except where otherwise specified, were added to the solution in the following order: wastewater, hydrogen peroxide and ferrous iron.

RESULTS AND DISCUSSION

Comparison of oxidation efficiencies of the electrode materials

Cathode efficiency is important for electrolysis systems. Various cathode materials have been thus far used in laboratory-scale or even pilot-scale experiments. Different electrode materials exhibit different decomposition abilities, which mainly depend on the electrode potential of organic compounds. Figure 1a illustrates the electrooxidation effects of different cathodes under the following conditions: pH 4, voltage of 12 V, current of 0.2 A, electrode space of 2 cm and treatment time of 60 min. The results illustrated in Figure 1a reveal that the oxidation ability of three stainless electrodes, two stainless electrodes, iridium–ruthenium alloy with stainless steel and iridium–ruthenium alloy with titanium mesh systems decreased successively. The results indicate that the stainless cathode performed more efficiently than the iridium–ruthenium alloy mesh and titanium mesh electrodes. Two stainless boards as cathode systems exerted the best oxidation effects for doubling the electrode area. Electrolysis with a stainless board electrode exhibited a stronger oxidative ability than those of iridium–ruthenium alloy and titanium mesh cathodes because of the production of Fenton reagents. The electrooxidation system with an iridium–ruthenium alloy mesh and a titanium mesh as electrodes exerted a slight oxidation effect on wastewater because system oxidation was achieved only by the electrode reaction and not by Fenton oxidation.

Meanwhile, there was no Fe²⁺ to produce by using the iridium–ruthenium alloy and titanium mesh as cathodes, which markedly decreased the

production of H_2O_2 in the electrolysis system.

Effect of supporting electrolytes on the oxidation system

An electrolyte improves the conductivity of the solution and accelerates electron transfer, facilitating electrolysis. Thus, a supporting electrolyte is necessary, particularly in a solution without sufficient conductivity. Figure 1b presents a comparison of the electro-Fenton system with and without supporting electrolytes. Other reaction conditions were as follows: pH 4, applied voltage of 12 V, current of 0.2 A, electrode space of 2 cm, and aeration. The results indicated that the COD_{cr} removal rate increased from 0.3% to 2.8% by adding 1 g/L NaCl as a supporting electrolyte in the iridium–ruthenium alloy with titanium mesh systems. A similar result was obtained in the iridium–ruthenium alloy with stainless electrode systems. The reason is that NaCl can not only increase the conductivity of wastewater, but also decrease the applied voltage and accelerate electrolysis. In addition, chlorine was produced by electrode reaction in the oxidation system because of the presence of Cl^- . Chlorine is soluble in water and changes into HClO , which facilitates the oxidative degradation of wastewater.

Effect of current density on the oxidation system

The applied voltage and current are directly related to the cost of the electro-Fenton process. With an increase in current, wastewater degradation initially increases and then stabilizes because of the side reactions and polarization. Current density in the electro-Fenton process is always low, which is a disadvantage of the

process because higher current density indicates a higher reaction rate.²⁰

The production of H_2O_2 through oxygen electrolysis requires sufficient current density and potential gradient. Meanwhile, current density also reflects the production rate of Fe^{2+} . The effect of current density on COD removal rate was confirmed under other treatment conditions: applied voltage of 12 V, current density of 76.6 A m^{-2} and electrode space of 2 cm.

As shown in Figure 2a, the COD removal rate increases continuously as current density increases. The reason is that $\cdot\text{OH}$ radicals are produced by high-concentration Fe^{2+} catalysis, which is provided by the high current density in the oxidation system. Considering operating costs, high current density leads to high energy consumption and low oxidation efficiency. Meanwhile, the high concentration of $\cdot\text{OH}$ radicals produced in the system is also involved in undesirable side reactions, causing invalid consumption of energy and chemicals. Thus, the optimal current density of the electro-Fenton system is 76.6 A m^{-2} .

Effect of pH on the oxidation system

Another important factor influencing the electro-Fenton process is the pH. The optimum pH level ranges from 2 to 5.¹⁹ The pH of wastewater may be reduced using two methods: by adding acid and by mixing the target wastewater with acidic wastewater. Several studies have investigated wastewater treatment at neutral pH and found that organics can also be removed successfully. However, in such a case, wastewater is treated mainly by the coagulation rather than by the degradation of OH^- .²¹

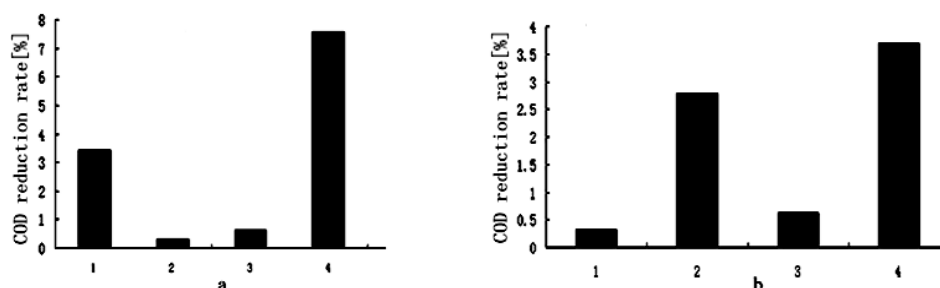


Figure 1: Effects of electrode materials and supporting electrolyte on the electro-Fenton system; a – 1. two stainless steel electrodes (anode and cathode), 2. iridium–ruthenium alloy (anode) and titanium mesh (cathode), 3. iridium–ruthenium alloy (anode) and stainless (cathode), 4. three stainless steel electrodes (two cathodes with one anode); b – 1. iridium–ruthenium alloy (anode) and titanium mesh (cathode), 2. iridium–ruthenium alloy (anode) and titanium mesh (cathode) with NaCl as electrolyte, 3. iridium–ruthenium alloy (anode) and stainless steel (cathode), 4. iridium–ruthenium alloy (anode) and stainless (cathode) with NaCl as electrolyte

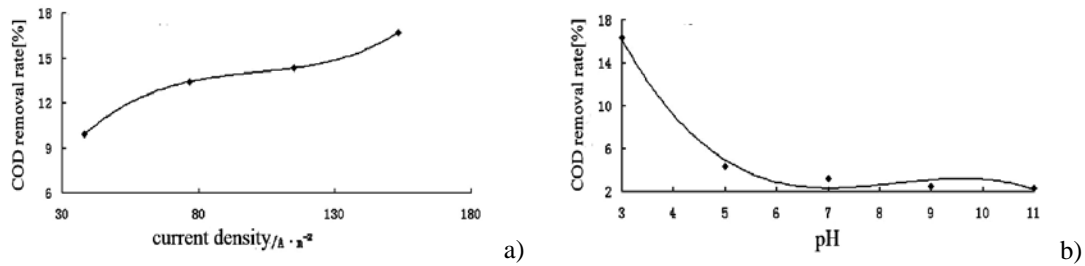


Figure 2: Influence of current density (a) and pH (b) on COD removal rate

In an alkaline solution, iron ions, particularly Fe^{3+} , precipitate. Consequently, the amount of catalyst in Fenton's reaction decreases. Meanwhile, if $pH < 2$, H_2O_2 cannot be decomposed into $\cdot OH$ by Fe^{2+} , which also lowers the oxidation efficiency. To confirm the optimal pH for the preimpregnated wastewater of CTMP, the COD removal efficiency at different pH levels was evaluated under the following conditions: applied voltage of 12 V, current density of $76.6 A \cdot m^{-2}$ and electrode space of 2 cm.

Figure 2b shows that the COD removal rate decreases as the pH value increases, particularly when $pH > 5$. The COD removal rate reached 16.3% when pH was 3, and the removal rate decreased to 4.3% when pH increased to 5. Although $\cdot OH$ was generated at pH 3 and under alkaline conditions, a higher $\cdot OH$ concentration was probably produced at pH 3 under the given experimental conditions. In addition, the lower COD removal rate under alkaline conditions was attributable to the lower $\cdot OH$ oxidation potential under alkaline conditions than under acidic conditions.²²

Effect of aeration on the oxidation system

In the electro-Fenton process, H_2O_2 is generated from oxygen reduction. The efficiency of aeration is important not only for the generation of H_2O_2 , but also for the operating cost.

The production of H_2O_2 may be improved using two methods: by selecting a cathode with a large surface area and by improving the aeration efficiency.

Tests were conducted to evaluate the influence of the supplied gas on the production of hydrogen peroxide and oxidation effects. Aeration exhibited an agitation effect on the oxidation system, which enhanced the effects of mass transfer, accelerated the reaction speed and increased the dissolved oxygen, which contributed to the production of H_2O_2 .

Table 1 shows the influence of aeration on COD removal rate under the following conditions: applied voltage of 12 V, current density of $76.6 A \cdot m^{-2}$, electrode space of 2 cm and reaction time of 30 min.

Table 1 illustrates that the aeration rate influences COD and turbidity removal. The COD removal rate slightly decreased as the aeration rate increased from $16 L \cdot h^{-1}$ to $80 L \cdot h^{-1}$. This reduction could be attributable to the gas flow obstacle, resulting from the low capacity of the reaction cell and broad electrode style, which reduced gas transfer in the reaction system. The turbidity removal rate exhibited a similar changing trend. The data in Table 1 suggest that the aeration capacity of $16 L/h$ is suitable in the experimental range.

Table 1
Influence of aeration rate on COD and turbidity removal rates

Aeration, $L \cdot h^{-1}$	Turbidity, NTU	Turbidity removal rate, %	COD, $mg \cdot L^{-1}$	COD removal rate, %
16	392	49.9	19600	40.1
40	418	46.6	20900	39.3
60	415	47.0	20750	39.0
80	407	48.0	20350	38.0

Note: Turbidity of raw wastewater was 783 NTU and COD – 33200 mg/L

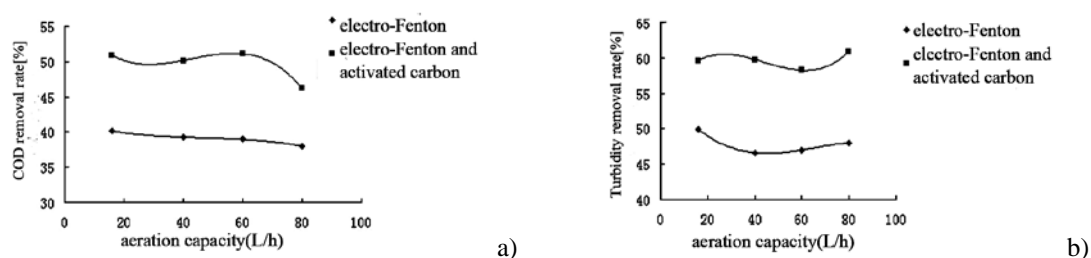


Figure 3: Comparative effects of electro-Fenton oxidation and electro-Fenton process followed by activated carbon adsorption on COD (a) and turbidity (b) removal rates

Electro-Fenton/activated carbon adsorption

To achieve an improved oxidation effect, activated carbon adsorption was employed. A comparison of the oxidation results between the Fenton process and the electro-Fenton process followed by carbon adsorption is presented in Figure 3a. The COD removal rate under electro-Fenton/carbon adsorption showed a significant increase relative to that of the electro-Fenton process alone. The coagulation conditions were as follows: pH 5 and aluminum sulfate dosage of 0.6 g/L. This step was followed by electro-Fenton oxidation under the following conditions: applied voltage of 12 V, current density of 76.6 A m^{-2} , electrode space of 2 cm and reaction time of 30 min. After electro-Fenton oxidation, activated carbon adsorption was conducted with an activated carbon dosage of 5 g/L and pH 4.

Figure 3 (a and b) illustrates the COD and turbidity removal by the electro-Fenton process and electro-Fenton/activated carbon adsorption. The COD removal rate achieved by the electro-Fenton/activated carbon adsorption exceeded that obtained by electro-Fenton oxidation by 10%, indicating that using two treatment methods exerted a positive synergistic effect.

Effect of electro-Fenton process on the biodegradability of wastewater

Various types of pollutants are found in papermaking wastewater, which contains high concentrations of lignin, cellulose and resin acid. These materials are difficult to degrade. To degrade refractory substances in wastewater, advanced oxidation technology has to be employed. Electrochemical treatment of mid-segment wastewater from papermaking can markedly improve its biodegradability.¹⁶ Therefore, electrochemical oxidation can be used not only as a separate treatment method, but also

as a pretreatment or post-treatment technique for the degradation of organic pollutants that exhibit poor biodegradability.^{17,19}

BOD/COD (B/C value) is an index for effluent biodegradability. If BOD/COD > 0.4, the effluent exhibits high biodegradability.²³ If BOD/COD < 0.3, the effluent exhibits low biodegradability. Table 2 reveals effluent BOD value of 65 mg L^{-1} , COD – of 437.7 mg L^{-1} and B/C – of 0.15. Under conventional Fenton oxidation, B/C increased to 0.39. Comparatively, B/C increased to 0.44 using electro-Fenton oxidation, indicating that the biodegradability of wastewater was markedly improved. The optimal conditions for electro-Fenton oxidation were as follows: electric current of 0.3 A, treatment time of 30 min, pH 3 and dosage of hydrogen peroxide of 0.025 mol/L.

The aforementioned results indicate that the electrochemical treatment can effectively treat high-concentration and hard-to-biodegrade papermaking wastewater.^{18,19} This technique has the following characteristics: it is not affected by water quality and quantity change, it requires a short processing time, and it improves the degradation or removal of some refractory toxic pollutants from papermaking wastewater. The wastewater chroma and turbidity decreased, the COD removal rate reached 85%, and B/C increased to 0.44, indicating the breakdown of organic compounds into biodegradable forms and the increase in biodegradability of papermaking wastewater achieved by the electro-Fenton process.¹⁹ The increase in biodegradability showed that the electro-Fenton process can efficiently treat wastewater from paper recovery industries. This wastewater is mainly composed of cellulosic and lignin compounds.¹⁹

Effects of various factors on organic pollutant components in the electro-Fenton process

The ether extract obtained from papermaking wastewater was evaluated only by GC/MS online.

The chromatographic peaks were qualitatively analyzed, the molecular structure of the groups was determined, the peak area was normalized and the relative content of the components was obtained with the aid of a software application. The results are listed in Table 3.

Table 3 lists the organic compounds detected in the wastewater obtained from a two-stage sedimentation tank: acids, alcohols, benzene, alkanes, phenols and ethers. The organic compounds with relative contents > 5% were 2,4-di-tert-butyl-phenol, hydrate terpene, 24 alkanes *etc.* Those with relative contents > 2% were diethyl phthalate, phenylacetic acid, 22 alkanes, coprostanol, 1-chloro twenty-seven alkane *etc.* The organic compounds with relative contents > 1% included phthalic acid, 2-ethylhexyl *etc.* The results of the analysis

indicate that the wastewater from the two-stage sedimentation tank contains various pollutants. The contents of phenols and acids, which are difficult to degrade, are considerably high.

Tables 3-7 present a comparison of the main components of organic pollutants in the wastewater under different electrochemical treatment conditions. The tables show that the composition of the components markedly changed after the electro-Fenton treatment. The macromolecular chain alkane was degraded, the content of phenol and quinone markedly decreased, and some benzene ring polymers broke open. These occurrences contributed to the decreases in chroma and turbidity of papermaking wastewater, which are also the main reasons for improving the biodegradability of wastewater.

Table 2
Effects of different treatments on B/C in wastewater

No.	Type of wastewater	B/C
1	Raw water	0.15
2	Fenton-oxidized water	0.39
3	Electro-Fenton-oxidized water	0.44

Table 3
Gas chromatographic analysis of wastewater

No.	Peak name	Retention time	Peak height	Peak area	Content, %
1	3,5-Dibutyl,4-hydroxy methylbenzene	20.718	74509.664	2895560.500	5.3405
2	Diethyl phthalate	21.257	72400.750	1629204.250	3.0048
3	2,4-Ditertiary butyl phenol	21.780	829690.688	28972054.000	53.4349
4	Palmitic acid	26.418	348822.219	3442200.000	6.3487
5	Phenylacetic acid	22.537	122986.82	1540693.375	2.8088
6	Hydrate terpene	23.653	174121.422	2957081	5.391
7	Diethyl phthalate	25.08	237246.984	2393478.5	4.3635
8	2,6-Syringol	27.510	142546.766	831812.125	1.5342
9	3-Ethoxy-4-methoxy anisole	28.818	147898.078	1544566.000	2.8487
10	4-Methoxy-3-chloroacetic acid benzaldehyde	29.797	21862.879	120333.266	0.2219
11	Phthalic acid	30.482	94639.133	607752.000	1.1209
12	3-Methoxy-4-hydroxy acetyl benzene	33.678	6332.344	51498.582	0.0950
13	3,4-Two methoxy benzyl alcohol	33.710	18646.096	94844.547	0.1749
14	Diallyl lipoid	34.382	5597.955	70008.828	0.1291
15	Twenty-one alkane	35.650	4780.438	215093.125	0.3967
16	Twenty-two alkane	36.980	5143.909	64041.484	0.1181
17	Twenty-six alkane	43.135	6109.296	182246.766	0.3323
18	Coprostanol	44.05	3085.628	234223.031	0.427

Table 4
Gas chromatographic analysis of wastewater

No.	Peak name	Retention time	Peak height	Peak area	Content, %
1	2,6-Diallyl quinone	21.508	2639.903	47928.465	3.2613
2	2,4-Ditertiary butyl phenol	21.762	20706.699	342164.688	23.2829
3	Hydrate terpene	23.885	64768.758	920029.125	7.6693
4	Diethyl phthalate	25.183	93285.133	640101.938	5.3358
5	Palmitic acid	26.443	102035.070	480606.969	4.0063
6	2-Phthalic acid, 2-ethyl hexyl ester	27.410	11524.360	116560.523	0.9716
7	2,6-Syringol	27.547	32292.836	230537.234	1.9217
8	Coprostane	28.222	60238.250	511741.000	4.2658
9	3-Ethoxy-4-methoxy anisole	28.833	25038.789	244576.344	2.0388
10	4-Methoxy-3-chloroacetic acid benzaldehyde	29.393	22192.949	149798.734	1.2487
11	Diallyl lipid	30.502	17722.240	96519.664	0.8046

Note: Wastewater treatment conditions: current – 0.3 A, treatment time – 30 min, pH 3, hydrogen peroxide concentration – 0.025 mol/L

Table 5
Gas chromatographic analysis of wastewater

No.	Peak name	Retention time	Peak height	Peak area	Content, %
1	2,6-Diallyl quinone	21.28	6002.436	101579.367	3.4346
2	2,4-Ditertiary butyl phenol	21.745	55073.750	850975.875	28.7731
3	Phenylacetic acid	22.47	17751.533	293179.938	9.9130
4	Hydrate terpene	23.41	33473.730	484052.719	16.3667
5	Palmitic acid	26.688	12012.081	82846.836	2.8012
6	2-Phthalic acid, 2-ethyl hexyl ester	27.657	8536.119	56089.383	1.8965
7	2,6-Syringol	27.87	24557.525	144783.719	4.8954
8	Coprostane	28.018	7401.909	61861.266	2.0916
9	4-Methoxy-3-acid benzaldehyde	29.098	9107.911	81950.219	2.7709

Note: Wastewater treatment conditions: current – 0.5 A, treatment time – 30 min, pH 3, hydrogen peroxide concentration – 0.025 mol/L

Table 4 presents the results of the degradation of the main organic components by electro-Fenton oxidation under optimal conditions. Compared with the relative contents of the components in the raw water, the relative content of 2,4-ditertiary butyl phenol decreased from 53.4349% to 23.2829%. The 3,5-dibutyl, 4-hydroxy methylbenzene peaks in the raw water disappeared. Similarly, the peaks of polymer alkanes (twenty-one alkanes, twenty-two alkanes, twenty-six alkanes *etc.*) disappeared. This finding indicates that the phenol components, esters, aldehydes, acids and other substances in the wastewater were degraded by the electro-Fenton oxidation treatment. The molecular-chain alkanes were decomposed into small molecular organic compounds.

Tables 4-7 show that the four groups of samples have basically similar composition. 2,4-Ditertiary butyl phenol has the highest content. The contents in the four group samples were of 23.2829%, 28.7731%, 28.666% and 29.8734%. These results indicate that the sample with the highest COD removal rate also degraded phenol most efficiently. The aforementioned tables reveal that the content of 2,4-ditertiary butyl phenol increases to 28.7731%, when the current is increased to 0.5 A. The content increases to 28.666% when the concentration of hydrogen peroxide is reduced to 0.015 mol/L. When the initial pH is increased to 6, the content of 2,4-ditertiary butyl phenol increases to 29.8734%. The highest removal efficiency of phenol from wastewater was achieved under the following

conditions: current of 0.3 A, treatment time of 30 min, pH 6 and hydrogen peroxide concentration of 0.025 mol/L. These results were consistent with the highest COD removal rate from wastewater achieved under the same treatment conditions.

FTIR analysis

The absorbance bands in the 1740-1701 cm⁻¹ region were attributed to the C=O stretching of the acetyl group or the ester linkage of the carboxylic group of lignins.²⁴⁻²⁷ As shown in Figure 4, the absorption of original wastewater is lower than that of the water treated by oxidation. This finding suggests that Fenton and electro-Fenton systems caused the breakage of ester linkages and long-chain structure of the wastewater.

The absorption at 1640 cm⁻¹ was attributed to the stretching vibration of conjugated carbonyl groups. Compared with wastewater treated with

Fenton oxidation, the wastewater treated with electro-Fenton oxidation exhibited a lower relative absorption, indicating that the number of the conjugated carbonyl groups was effectively reduced with the electro-Fenton treatment. The absorption at 1576 cm⁻¹ was associated with the aromatic skeleton vibration and C=O stretching vibration. The data in Figure 4 show that the wastewater treated with Fenton oxidation and electro-Fenton oxidation has a lower relative absorption, indicating that oxidation may decompose the aromatic ring.

The absorption bands at 1123 and 1033 cm⁻¹ were associated with the ether bonds of lignins. The absorption values of the wastewater treated with Fenton oxidation and electro-Fenton oxidation suggest that electro-Fenton oxidation increased the fracture of the ether bonds.

Table 6
Gas chromatographic analysis of wastewater

No.	Peak name	Retention time	Peak height	Peak area	Content, %
1	2,6-Diallyl quinone	21.303	5923.792	111511.406	4.0582
2	2,4-Ditertiary butyl phenol	21.773	47539.012	787684.063	28.6660
3	Phenylacetic acid	22.493	16221.945	274746.500	9.9988
4	Palmitic acid	26.7	11647.103	87693.336	3.1914
5	2,6-Syringol	27.67	8428.376	54862.727	1.9966
6	2-Phthalic acid, 2-ethyl hexyl ester	27.883	23712.648	145025.250	5.2779
7	Coprostane	28.033	7109.554	59809.609	2.1766
8	4-Methoxy-3-chloroacetic acid benzaldehyde	29.115	8855.824	80168.016	2.9175

Note: Wastewater treatment conditions: current – 0.3 A, treatment time – 30 min, pH 3, hydrogen peroxide concentration – 0.015 mol/L

Table 7
Gas chromatographic analysis of wastewater

No.	Peak name	Retention time	Peak height	Peak area	Content, %
1	2,4-Ditertiary butyl phenol	21.783	34094.813	757948.125	29.8734
2	Phenylacetic acid	22.505	13012.368	234448.766	9.2405
3	Hydrate terpene	23.452	25466.775	389227.938	15.3409
4	Palmitic acid	26.733	13224.258	85376.172	3.3650
5	2,6-Syringol	27.7	13243.585	73748.438	2.9067
6	2-Phthalic acid, 2-ethyl hexyl ester	27.915	41827.301	211275.250	8.3271
7	3-Ethoxy-4-methoxy anisole	28.06	8363.007	69650.125	2.7452
8	4-Methoxy-3-chloroacetic acid benzaldehyde	29.135	15799.873	111241.039	4.3844

Note: Wastewater treatment conditions: current – 0.3 A, treatment time – 30 min, pH 6, hydrogen peroxide concentration – 0.025 mol/L

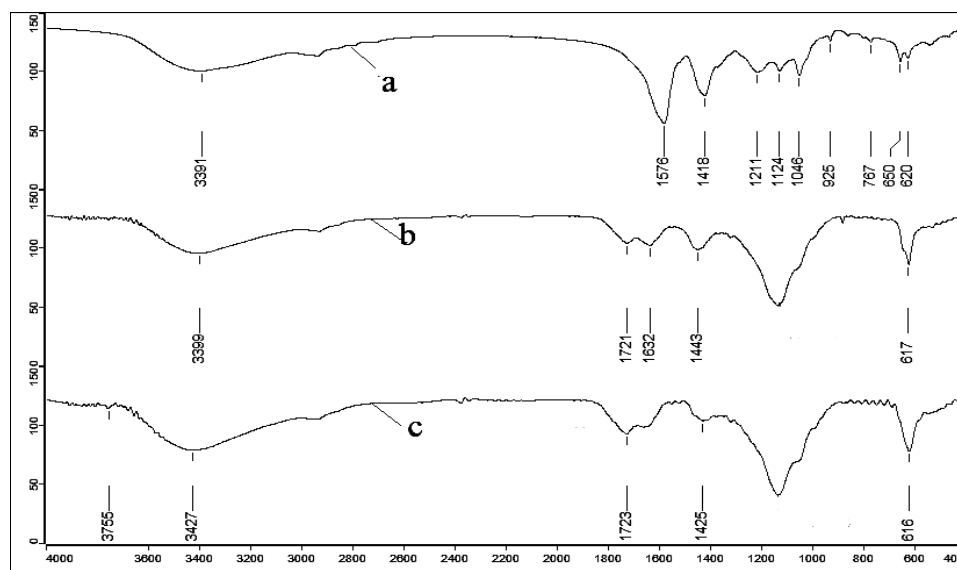


Figure 4: Infrared spectra of CTMP wastewater after different treatments; a – raw wastewater, b – Fenton-oxidized water, c – electro-Fenton oxidized water

The absorption bands at 925 and 874 cm^{-1} , which were associated with the anomeric carbon vibration of cellulose and hemicellulose, disappeared. This occurrence indicates the degradation of cellulose and hemicellulose. Compared with Fenton oxidation, electro-Fenton oxidation degraded cellulose and hemicellulose further, suggesting stronger oxidation achieved by the electro-Fenton system.

The presence of various functional groups in the FTIR spectra confirmed the complexity of the wastewater.¹⁶ The presence of these organic pollutants in wastewater revealed the breakdown of chemical bonds and enhanced biodegradability, which contributed to the decrease in COD, BOD and turbidity of wastewater.

CONCLUSION

To increase the oxidizing ability of Fenton reagents and reduce the reagent costs involved in Fenton oxidation, the electro-Fenton process was employed for the degradation of hard-to-treat CTMP wastewater. The removal rates of COD_{cr} and turbidity of preimpregnation wastewater of chemithermomechanical pulping under the effect of electro-Fenton oxidation were investigated. The results indicated that the optimal electro-Fenton oxidation conditions were as follows: pH 4, applied voltage of 12 V, current of 0.2 A, electrode space of 2 cm and aeration gas flow of 16 L/h. The COD_{cr} removal rate reached 40.1% and the turbidity removal rate was 49.9% under the aforementioned electro-Fenton process.

FTIR analysis suggested that, compared with Fenton oxidation, electro-Fenton oxidation exhibited a greater degradation ability for the preimpregnated wastewater of CTMP.

ACKNOWLEDGMENT: This study was financially supported by the National Natural Science Foundation of China (No. 31470606).

REFERENCES

- 1 M. Ali and T. R. Sreekrishnan, *Adv. Environ. Res.*, **5**, 175 (2001).
- 2 R. M. Billings and G. G. DeHaas, "Industrial Pollution Control Handbook", edited by H. F. Lund, McGraw-Hill, New York, 1971, pp. 18-28.
- 3 R. Crooks and J. Sikes, *Appita J.*, **43**, 67 (1991).
- 4 D. Reeve, *Tappi J.*, **74**, 123 (1991).
- 5 M. Kamali and Z. Khodaparast, *Ecotoxicol. Environ. Saf.*, **326**, 114 (2015).
- 6 G. Sundman, T. K. Kirk and H. M. Chang, *Tappi J.*, **64**, 45 (1981).
- 7 T. H. Kim, C. Park, J. Lee, E. B. Shin and S. Kim, *Water Res.*, **36**, 3979 (2002).
- 8 R. Pelegrini, P. Peratte-Zamore, A. R. De Andrade, J. Reyes and N. Daran, *Appl. Catal. B-Environ.*, **22**, 83 (1999).
- 9 A. G. Vlyssides, D. Papaioannou, M. Loizidou, P. K. Karlis and A. A. Zorpas, *Waste Manag.*, **20**, 569 (2000).
- 10 K. Eskelinen, H. Särkkä, T. A. Kurniawan and M. E. T. Sillanpää, *Desalination*, **255**, 179 (2010).
- 11 K. Juttner, U. Galla and H. Schmieder, *Electrochim. Acta*, **45**, 2575 (2000).
- 12 C. C. Jiang and J. F. Zhang, *J. Zhejiang Univ. Sci.*

A, **8**, 1118 (2007).

¹³ M. A. Oturan, *J. Appl. Electrochem.*, **30**, 475 (2000).

¹⁴ N. Jaafarzadeh, F. Ghanbari, M. Ahmadi and M. Omidinasab, *Chem. Eng. J.*, **308**, 142 (2017).

¹⁵ A. Altin, S. Altin and O. Yildirim, *J. Environ. Protect. Ecol.*, **18**, 652 (2017).

¹⁶ S. Y. Guvenc, H. S. Erkan, G. Varank, M. S. Bilgili and G. O. Engin, *Water Sci. Technol.*, **76**, 2015 (2017).

¹⁷ G. Moussavi and M. Aghanejad, *Sep. Purif. Technol.*, **132**, 182 (2014).

¹⁸ F. L. Zhang, G. M. Li, X. H. Zhao, H. K. Hu and J. W. Huang, *Ind. Water Treat.*, **24**, 9 (2004).

¹⁹ Z. Chen, X. Chen, X. Zheng, R. Y. Chen, Z. H. Lin,

Y. F. Chen and Y. K. Zhang, *Res. Environ. Sci.*, **15**, 42 (2002).

²⁰ A. Babuponnusami and K. Muthukumar, *Clean Soil Air Water*, **39**, 142 (2011).

²¹ Y. C. Hsu, H. C. Yang and J. H. Chen, *Chemosphere*, **56**, 149 (2004).

²² N. Sgriccia, M. Hawley and M. Misra, *Compos. Part A*, **39**, 1632 (2008).

²³ V. Tserki, N. E. Zafeiropoulos, F. Simon and C. Panayiotou, *Compos. Part A*, **36**, 1110 (2005).

²⁴ A. Alemdar and M. Sain, *Bioresour. Technol.*, **99**, 1664 (2007).

²⁵ Q. Zhao, Z. H. Wang, X. J. Jin, D. Z. Sun, T. T. Jiang *et al.*, *Cellulose Chem. Technol.*, **48**, 745 (2014).